An h*Per2* Phosphorylation Site Mutation in Familial Advanced Sleep Phase Syndrome

Kong L. Toh,[1]* Christopher R. Jones,[2,3]* Yan He,[4] Erik J. Eide,[5] William A. Hinz,[5] David M. Virshup,[5,6] Louis J. Ptáček[2,7]† Ying-Hui Fu[4]

Familial advanced sleep phase syndrome (FASPS) is an autosomal dominant circadian rhythm variant; affected individuals are "morning larks" with a 4-hour advance of the sleep, temperature, and melatonin rhythms. Here we report localization of the FASPS gene near the telomere of chromosome 2q. A strong candidate gene (h*Per2*), a human homolog of the *period* gene in *Drosophila*, maps to the same locus. Affected individuals have a serine to glycine mutation within the casein kinase Iε (CKIε) binding region of hPER2, which causes hypophosphorylation by CKIε in vitro. Thus, a variant in human sleep behavior can be attributed to a missense mutation in a clock component, hPER2, which alters the circadian period.

The identification of genes influencing any aspect of human behavior is complicated by other genetic influences, behavioral tendencies, and cultural factors. We recently described a familial abnormality of human circadian behavior that segregates in a highly penetrant autosomal dominant manner and produces a striking 4-hour advance of the daily sleep-wake (*1*) rhythm. In this behavioral trait, known as familial advanced sleep phase syndrome (FASPS), sleep onset occurs at approximately 7:30 p.m., when most people are actively socializing. Sleep duration is normal but is terminated by a spontaneous awakening at approximately 4:30 a.m., just when conventional sleepers are at their sleepiest time of the 24-hour cycle.

Biological "clocks" that free-run in constant conditions with an endogenous period (τ) close to the 24-hour period of the solar day are ubiquitous among eukaryotes and provide important adaptational advantages by anticipating the transitions between night and day (*2*). The mammalian circadian pacemaker resides in the paired suprachiasmatic nuclei (SCN) and influences a multitude of biological processes, including the sleep-wake rhythm (*3*). The core clock mechanism in the SCN interacts with other brain regions to form a circadian system that is entrained primarily by ambient light levels. Although the timing of sleep is strongly influenced by

the circadian system, other factors such as social schedules and previous sleep deprivation may predominate.

Mutagenesis screens in animals and recognition of spontaneous mutations led to the discovery of short and long τ autosomal semidominant circadian rhythm mutants in fungi, plants, *Drosophila*, and rodents (*2*, *4*, *5*). Long period mutants are generally found to be phase-delayed with respect to an entraining light-dark cycle, whereas short τ mutants are usually phase-advanced (*6*). Genetic study of these abnormal circadian phenotypes led to the identification and characterization of clock genes responsible for circadian behavior (*2*, *4*, *5*, *7*). The encoded proteins function in interacting feedback loops composed of PAS (PER-ARNT-SIM) domain transcription factors that are both negatively and positively controlled by regulatory phosphoproteins such as PERIOD and CRYPTOCHROME (*8*).
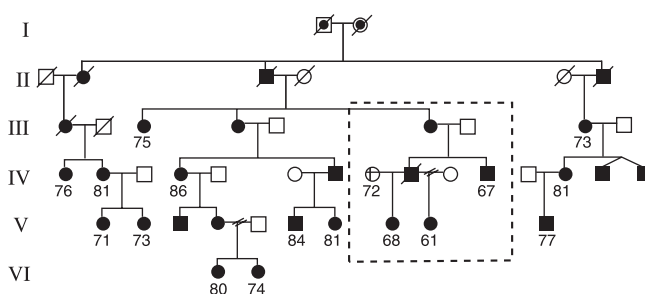
To determine the genetic basis of FASPS, linkage analysis was performed in a large family segregating an FASPS allele (K2174) (Fig. 1). Previously described strict criteria for classification of patients with FASPS were used (*1*). All participants filled out the

Horne-Östberg questionnaire, a validated tool for evaluation of an individual's tendency between the extremes of "morning lark" (scores, 70 to 86) to "night owl" (scores, 16 to 30) (*1*, *9*). In the initial automated genome-wide scan, highly polymorphic tetranucleotide and dinucleotide repeat markers, distributed every ~20 cM across the genome, were chosen for the mapping set (*10*). Linkage analysis revealed a number of small positive lod (logarithm of the odds ratio for linkage) scores. These were examined by polymerase chain reaction (PCR) amplification of genomic DNA from all members of kindred 2174 with additional markers spanning these loci (*11*).

A maximum lod score of ~3 was identified for marker D8S366, but extensive genotyping of this region revealed this to be a false positive (*12*). An examination of telomeric markers for each chromosome (because the high rate of recombination at telomeres may have obscured linkage with the initial marker set) revealed a single marker, D2S395, on chromosome 2qter that was linked to FASPS in kindred 2174 (maximum lod score of 5.25 at θ = 0.00). Simultaneously, an additional set of 400 genome-wide markers from the ABI PRISM LMS-MD10 Linkage Mapping set was used to expand the genome-wide coverage to 600 markers spaced at an average of 7-cM intervals. D2S125, the marker in this set nearest to D2S395, had a maximum lod score of 1.75 at θ = 0.10 but, otherwise, analysis of this data set did not reveal any other loci with significant lod scores. We also performed manual linkage analysis with seven additional markers previously localized to a 19-cM region of chromosome 2qter (*13*, *14*). Evaluation of K2174 with the additional markers yielded a maximum lod score of 3.81 at θ = 0.05. For each of these markers, we found that individuals initially classified as affected in branch 3 carried a different allele than the one segregating with ASPS in the rest of the family (Fig. 1). The haplotype generated using these markers cosegregated with ASPS in all affected individuals of K2174 except those in branch 3.

A homolog (h*Per2*) of the *Drosophila period* gene resides on chromosome 2qter and is an excellent candidate gene for FASPS. Of the

[1]Department of Human Genetics, [2]Department of Neurology, [3]University Hospital Sleep Disorders Center, [4]Department of Neurobiology and Anatomy, [5]Department of Oncological Sciences and the Huntsman Cancer Institute Center for Children, [6]Department of Pediatrics, [7]Howard Hughes Medical Institute, University of Utah, Salt Lake City, UT 84112, USA.

*These authors contributed equally to this work.
†To whom correspondence should be addressed. E-mail: ptacek@genetics.utah.edu

Fig. 1. ASPS kindred 2174. Horne-Östberg scores are shown below individuals. The dotted line marks a branch (branch 3) where the ASPS phenotype does not cosegregate with the mutation. Circles, women; squares, men; filled circles and squares, affected individuals; empty circles and squares, unaffected individuals. Unknown individuals (not meeting strict criteria for being "affected" or "unaffected") were eliminated from this pedigree for the sake of simplicity.

three human *period* homologs, h*Per2* is the most similar to d*per* (*15*). In addition, mutations in *Per* in the fly (*16*) and in the mouse (m*Per*) (*17*) produce a similar short period phenotype. In humans (and other animals), short period mutations are predicted to phase-advance circadian rhythms under entrained conditions (*18, 19*). Furthermore, unlike m*Per1* and m*Per3*, the phase response curve for light induction of m*Per2* RNA is maximal at CT 14 (*20*) when phase delays are elicited by light. This is consistent with a predominantly phase delay function for mPER2. Thus, a loss-of-function mutation in hPER2 could, theoretically, lead to a phase advance.

The localization of h*Per2* on chromosome 2qter was confirmed by isolating a BAC clone (552H8, CITB human BAC library) containing the h*Per2* gene for use in fluorescence in situ hybridization experiments (*21*). This BAC mapped to the tip of chromosome 2q (*12*). In addition, we used a polymorphism in h*Per2* to genotype K2174 and performed two-point linkage mapping with nine markers noted previously (*13*). A recombination demonstrated the h*Per2* gene to be distal to marker D2S338. The haplotype of the remaining eight markers was fully linked to h*Per2* in this family. The individuals in branch 3 were considered to represent phenocopies, and mutation analysis of h*Per2* was performed.

Human *Per2* comprises 23 exons (Fig. 2A) (*22*). A sequencing error of the h*Per2* cDNA (GenBank accession number, NM 003894) was identified; the reported cDNA has a missing base at position 3652 that shifts the reading frame, predicting translation of 69 amino acids that are not homologous to other PER proteins before the stop codon. With the corrected sequence, the region 3′ of that base encodes 78 amino acids that are 64% identical to mPER2.

Single-strand conformation polymorphism (SSCP) analysis (*23*) of affected and unaffected individuals revealed a complex banding pattern in exon 17. Sequencing of this exon from individuals in K2174 revealed four changes. Three of the four changes [base pair 2087 (bp2087) A/G, bp2114 A/G, and bp2117 A/G] occur at wobble positions and, therefore, preserved the amino acid sequence. However, the base change at position 2106 (A to G) of the h*Per2* cDNA predicts substitution of a serine at amino acid 662 with a glycine (S662G) (Fig. 2). This change was not found in 92 controls. The S662G change cosegregates with the ASPS phenotype in this family, except for the branch in which the FASPS-associated marker alleles were unlinked (Fig. 1). Four additional at-risk individuals in the family carry the mutation but did not meet strict affection criteria, although they did show a strong tendency of early sleep-wake preference (Horne-Östberg scores 74.4 ± 7.2; *n* = 4) (*1*).

To establish whether this mutation causes FASPS, the S662G mutation was functionally characterized (*24*). To determine whether S662 is located within the CKIε binding site of hPER2, CKIε, myc-epitope tagged mPER2, and the indicated truncation mutants of mPER2 (Fig. 3) were expressed in rabbit reticulocyte lysates and mPER2 peptides were immunoprecipitated with antibodies to myc (*25*). CKIε was coprecipitated with mPER2(1 to 763) but not mPER2(1 to 554), thus demonstrating that the CKIε binding site of mPER2 is located between residues 554 and 763, corresponding to residues 556 to 771 of hPER2 (Fig. 3).

Studies of *doubletime* (*dbt*) mutants in *Drosophila* (*26*) and the *tau* mutant in the golden hamster (*27*) indicate that mutations affecting the function of CKIε disrupt endogenous circadian clock function leading to altered period lengths or arrhythmicity. In addition, hPER2 and mPER2 are substrates of CKIε. Because the S662G mutation is located within the CKIε binding region, hPER2 and mPER2 fragments extending from amino acids 474 to 815 and 472 to 804, respectively, were used to evaluate the effect of the mutation on PER2 phosphorylation (*28*). To test whether the S662G mutation eliminates a potential phosphorylation site, reticulocyte lysates containing ³⁵S-labeled hPER2 fragments were incubated with a low concentration of CKIε (0.25 ng/μl). An electrophoretic mobility shift was observed when wild-type (S662) but not mutant (G662) fragments were treated with CKIε (Fig. 4A). A similar result was obtained with wild-type and mutant mPER2 fragments (*12*). Phosphatase treatment confirmed that this shift was due to phosphorylation (Fig. 4). When the experiment was repeated with a higher concentration of CKIε (6.5 ng/μl), mobility shifts were observed for both the wild-type and mutant hPER2 fragments (Fig. 4B). Thus, regardless of the phosphorylation status of S662, other residues in the peptide can be phosphorylated with excess kinase.

CKIε preferentially phosphorylates peptides with acidic [for example, DDDD-X-X-S] or phosphorylated residues [for example, S($\overline{\text{P}}$)-X-X-$\underline{\text{S}}$] immediately upstream of the target residue (where D is aspartate, S is serine, S(P) is a phosphoserine, X is any amino acid, and the underlined "S" is the target of the subsequent phosphorylation) (*29, 30*). Analysis of the hPER2 sequence reveals four additional serine
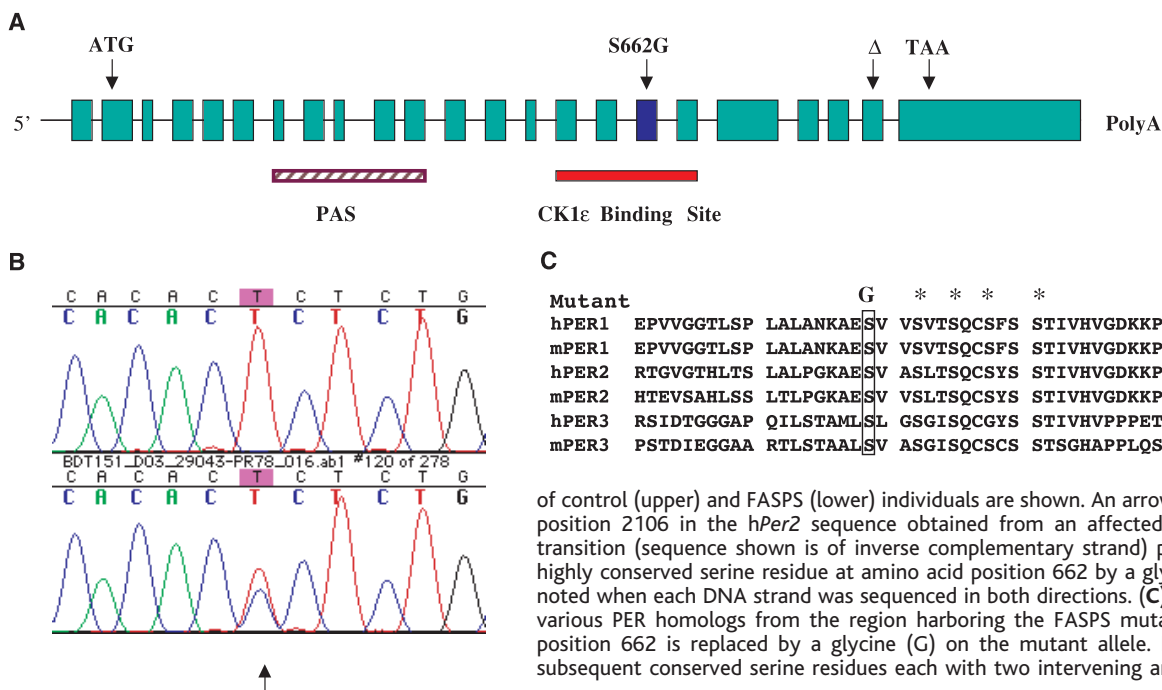

Fig. 2. (A) Genomic structure of h*Per2*. The h*Per2* gene contains 23 exons (colored rectangles). The intervening introns are not drawn to scale. The mutation in kindred 2174 (S662G) occurs in exon 17. The "Δ" above exon 22 shows the location of the sequence error (a 1 base pair deletion) in the h*Per2* cDNA GenBank sequence. **(B)** The h*Per2* mutation in kindred 2174. DNA sequences from the h*Per2* gene of control (upper) and FASPS (lower) individuals are shown. An arrow marks a double peak at position 2106 in the h*Per2* sequence obtained from an affected individual. This A to G transition (sequence shown is of inverse complementary strand) predicts substitution of a highly conserved serine residue at amino acid position 662 by a glycine. A double peak was noted when each DNA strand was sequenced in both directions. **(C)** Amino acid sequence of various PER homologs from the region harboring the FASPS mutation (*37*). The serine at position 662 is replaced by a glycine (G) on the mutant allele. Four asterisks mark four subsequent conserved serine residues each with two intervening amino acids.

residues, COOH-terminal to S662, which follow the pattern S-X-X-S (Fig. 2C). We speculated that after S662 is phosphorylated, it would create a CKIε recognition site facilitating the phosphorylation of S665, and so on. This entire series of serines could, therefore, be modified by CKIε after S662 is phosphorylated in a cascade of subsequent phosphorylations, as described previously for phosphorylation of p53 by CKI (Fig. 4A) (*31*, *32*).

To test this idea further, we mutated the serine residue at position 662 to aspartate, reasoning that the presence of a negative charge from the acidic residue would mimic a phosphoserine. Supporting this hypothesis, the CKIε-dependent phosphorylation was restored in the S662D mutant (Fig. 4C). At levels of CKIε that were not sufficient to cause a mobility shift in the S662G protein, both wild-type and S662D hPER2 had robust mobility shifts. Therefore, phosphorylation of S662 may regulate the subsequent phosphorylation of a series of downstream residues.

Interactions between PER2 and CKIε also provide a strong rationale for h*Per2* being

involved in the molecular pathogenesis of FASPS. In a current mammalian clock model, mPER2 is a positive regulator of the *Bmal1* feedback loop, raising the possibility that phase-advance of h*Per2* could phase-advance the feedback loop (*8*). Semidominant mutations in CKIε can advance activity phases and shorten τ in *Drosophila* and hamster (*26*, *27*). The *tau* R178C mutation substitutes cysteine for arginine in an anion-binding pocket on the structure of the kinase, potentially decreasing the ability of the hamster kinase to recognize acidic or phosphorylated residues that define the CKI recognition motif (*27*). Thus, the *tau* mutation may decrease phosphorylation of PER residues downstream of S662 due to diminished recognition of phosphoserine 662, and the FASPS mutation S662G mirrors this effect by preventing phosphorylation of residue 662.

Taken together, the *dbt* and *tau* mutant CKIε and the FASPS mutation in hPER2 suggest that one critical function of CKIε is to phosphorylate hPER2. However, we do not yet

fully understand the functional consequences of hPER2 phosphorylation. Phosphorylation of PER by CKI may promote its degradation during the circadian cycle (*25*, *26*, *33*, *34*). Deficient phosphorylation of hPER2 in the cytoplasm could impair its degradation and/or accelerate its nuclear entry and thus hasten its accumulation. This would phase-advance the rhythm of h*Per2*, perhaps in part by increasing transcription of *Bmal1* (*8*). The net result might be a shortening of τ and an advance of the sleep-wake rhythm, as seen in FASPS. It is also possible that the mutation affects not only period length, but also clock-output coupling.

Study of other FASPS families in our database demonstrated that some are unlinked to the h*Per2* locus, thus establishing the existence of locus heterogeneity in FASPS (*12*). Additional h*Per2* mutations in other ASPS probands were not identified. It is possible that we have missed mutations in intronic DNA that lead to alterations of h*Per2* expression. Short-period animal models caused by mutations in other genes, along with our failure to find other h*Per2* mutations in FASPS kindreds, predict that additional FASPS genes remain to be identified.

The following lines of evidence support the conclusion that the S662G mutation is responsible for FASPS in this family: (i) the FASPS allele in K2174 is linked to chromosome 2qter with significant lod scores despite the recombinant branch, (ii) h*Per2* is a physiologically relevant gene on chromosome 2qter and harbors the S662G mutation in all affected and genetically linked individuals, (iii) genome-wide linkage analysis with 600 markers spaced at average intervals of 7 cM did not identify another linked locus, (iv) the S662G mutation was not found in a large number of control chromosomes, and (v) the mutation leads to decreased phosphorylation by a kinase (CKIε) that, when mutated, causes a similar phenotype in *Drosophila* and the golden hamster. Taken together, these data demonstrate that h*Per2* is an ortholog of the d*per* gene and is a physiologically relevant target of CKIε, providing the first direct link between human clocks and those of model systems. The ASPS individuals in branch 3 did not carry the S662G mutation and therefore represent phenocopies of the ASPS phenotype (*35*).

The recognition that Mendelian circadian rhythm mutations occur in humans predicts that the elements of the human clock can now be systematically dissected. Other families in which an FASPS allele is not cosegregating with h*Per2* will provide an opportunity to identify mutations in other genes that lead to alterations of human circadian rhythms. Such discoveries will likely provide insights into human sleep and may ultimately improve our ability to treat not only ASPS, but also other sleep-phase disorders such as sleep-phase delay, ASPS of aging, jet-lag, and shift work.

Fig. 3. Mapping of the CKIε binding domain of PER2. CKIε, myc-epitope–tagged mPER2, and the indicated truncation mutants of mPER2 (lanes 1 to 6) were expressed in rabbit reticulocyte lysates in the presence of ^{35}S-methionine, as described (*25*). Lysates containing CKIε were mixed with the indicated mPER2 construct, incubated for 60 min at 30°C, and the mPER2 protein immunoprecipitated. The presence or absence of co-immunoprecipitating CKIε was assessed by SDS-PAGE and PhosphorImager analysis (lanes 7 to 11). The

CKIε binding sites on mPER1 and mPER2 are 51% identical. The light gray bars indicate regions of homology to the cytoplasmic localization domain (CLD) of d*per*.
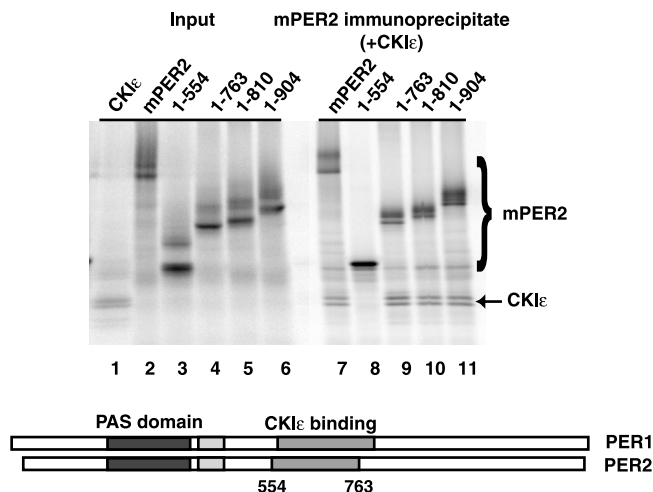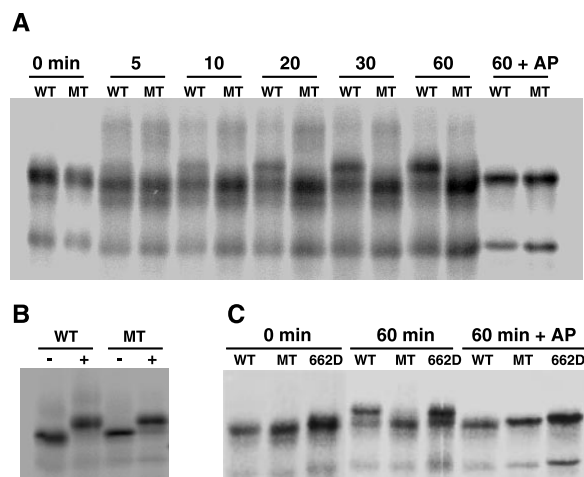
Fig. 4. In vitro CKIε phosphorylation of wild-type and mutant hPER2. In vitro transcribed and translated hPER2 (WT), mutant S662G (MT), and S662D were incubated with purified CKIε at 0.25 ng/μl in (**A**) and (**C**) and at 6.5 ng/μl in (**B**). Times at which reactions were terminated are shown. + AP, alkaline phosphatase added at the end of the reaction; −, no CKIε added; +, CKIε added.

References and Notes

1. C. R. Jones *et al.*, *Nature Med.* **5**, 1062 (1999).
2. J. C. Dunlap, *Cell* **96**, 271 (1999).
3. D. R. Weaver, *J. Biol. Rhythms* **13**, 100 (1998).
4. S. M. Reppert, *Neuron* **21**, 1 (1998).
5. D. P. King and J. S. Takahashi, *Annu. Rev. Neurosci.* **23**, 713 (2000).
6. M. J. Hamblen-Coyle *et al.*, *J. Insect Behav.* **5**, 417 (1992).
7. K. Wager-Smith, S. A. Kay, *Nature Genet.*, **26**, 23 (2000).
8. L. P. Shearman *et al.*, *Science* **288**, 1013 (2000).
9. Individuals who did not meet either the conservative affected or unaffected criteria were classified as unknown. Venous blood samples were gathered from individuals from ASPS families who were likely to contribute to linkage information. Participants signed a "Consent of Participation" form, which was approved by the Institutional Review Board for Human Research at the University of Utah School of Medicine. High–molecular weight genomic DNA was isolated from whole-blood lysates, and lymphoblastoid cell lines were transformed with Epstein-Barr virus, as described (*36*).
10. The fluorescently labeled markers were used to amplify genomic DNA in total reaction volumes of 20 μl in a MJR PTC-200 thermocycler (MJ Research, Watertown, MA). The products were visualized on an Applied Biosystems model 377 and analyzed by the Genotyper peak-calling software. Pairwise two-point linkage analysis with MLINK of the LINKAGE program was used. Disease penetrance was set at 0.95, without a gender difference, and the normal and FASPS allele frequencies were set at 0.999 and 0.001, respectively.
11. Manual genotyping was carried out after PCR of DNA samples with appropriate primers, as previously described (*36*).
12. K. L. Toh *et al.*, data not shown.
13. Markers D2S338, D2S2338, D2S2285, D2S2253, D2S125, D2S395, D2S140, D2S2986, and D2S2987 (from centromere to telomere) were used for genotyping and haplotype analysis.
14. C. Dib *et al.*, *Nature* **380**, 152 (1996).
15. U. Albrecht *et al.*, *Cell* **91**, 1055 (1997).
16. R. J. Konopka, S. Benzer, *Proc. Natl. Acad. Sci. U.S.A.* **68**, 2112 (1971).
17. B. Zheng *et al.*, *Nature* **400**, 169 (1999).
18. E. B. Klerman *et al.*, *Am. J. Physiol.* **270**, R271 (1996).
19. J. Duffy *et al.*, Sleep **22**, S92 (1999).
20. M. J. Zylka *et al.*, *Neuron* **20**, 1103 (1998).
21. Human lymphoblast cultures were treated with cholcimid (0.025 mg/ml) at 37°C for 1.5 hours. Coloemid treated cultures were pelleted at 500*g* at room temperature for 8 min. Pellets were then resuspended with 0.075M KCl (3 ml per pellet) for 15 min at room temperature. Cells were then fixed in 3:1 MeOH: acetic acid and stored at 4°C. Human bacterial artificial chromosomes (BACs) were labeled with spectrum orange using a nick translation kit per the manufacturers protocol (Vysis, Downers Grove, IL). Slides were prepared by dropping fixed cells onto glass slides and washing with excess fixative. The slides were then washed in acetic acid for 35 min at room temperature and were dehydrated for 2 min each in 70, 85, and finally 100% EtOH. Chromosomes were denatured in 70% formamide in 2×SSC at 74°C for 5 min, and slides were dehydrated again as above except in ice-cold EtOH. Two micrograms of labeled probe was blocked with 2 μg of human Cot-1 DNA in Hybrisol VI (ONCOR, Gaithersburg, MD). The probe mixture was denatured at 74°C for 5 min and then pre-annealed at 37°C for 15 min. Twelve microliters of pre-annealed probe was applied per slide, a cover slip was added, and edges were sealed with rubber cement. Slides were hybridized in a darkened, humidified chamber for 16 hours at 37°C. Hybridized slides were then washed in 0.4× SSC containing 0.1% Tween-20 at 74°C for 2 min, and then 1 min at room temperature in 2× standard saline citrate (SSC). Slides were allowed to dry in the dark at room temperature and were stained with 4′,6′-diamidino-2-phenylindole (DAPI) (Vector labs, Burlingame, CA) for chromosome visualization.
22. The h*Per2* intron-exon boundaries were determined in order to carry out the mutational analysis. Intron-exon boundaries of the h*Per2* gene were obtained by a combination of direct sequencing of h*Per2* BAC DNA and sequencing of PCR products from genomic DNA with primers distributed along the entire cDNA. Intronic sequence of at least 100 base pairs flanking each exon boundary was obtained. Intron sizes were determined directly from genomic sequence or estimated by the size of PCR products amplified using oligonucleotides from adjacent exons. All sequencing reactions were carried out with an Applied BioSystems model 377 DNA sequencer (Foster City, CA).
23. SSCP was carried out as described (*36*). PCR products were diluted, denatured, and electrophoresed through acrylamide gels and visualized on x-ray film at −80°C for 12 to 24 hours. Aberrant SSCP bands were cut directly from the dried gels and sequenced as described (*36*).
24. Complementary DNA clones encoding m*Per2* and h*Per2* were PCR amplified from the corresponding plasmids and cloned into the pCS2 + MT (myc-epitope tagged) vector as previously described (*25*). Site-directed mutagenesis of the serine residue at position 662 of hPER2 and the homologous serine (659) of mPER2 were performed to substitute a glycine residue. Mutagenesis was carried out with the QuikChange Site-directed Mutagenesis Kit (Stratagene) using the protocol outlined therein. Eco RI–Xba I fragments encoding amino acids 474 to 815 of hPER2 (and the corresponding amino acids 472 to 804 of mPER2) were PCR-amplified with primers containing Eco RI and Xba I sites, gel-purified with the GENECLEAN kit (BIO 101, Vista, CA) and were directionally cloned into the Eco RI–Xba I sites of the pCS2 + MT vector. Expression from an SP6 promoter generates 6-myc-tagged peptides. A series of 3′ deletion mutations of m*Per2* were constructed (encoding amino acids 1 to 554, 1 to 763, 1 to 810, and 1 to 904) for use in mapping the binding site for CKIε, as previously described for m*Per1* (*25*). All constructs were confirmed by sequencing.
25. E. Vielhaber *et al.*, *Mol. Cell. Biol.* **20**, 4888 (2000).
26. B. Kloss *et al.*, *Cell* **94**, 97 (1998).
27. P. L. Lowrey *et al.*, *Science* **288**, 483 (2000).
28. Transcription and translation of h*Per2* and m*Per2* inserts were performed in vitro in the presence of ³⁵S-methionine with the TnT SP6 Coupled Reticulocyte Lysate System (Promega) over a period of 90 min at 30°C. The labeled products were incubated with CKIε in buffer containing phosphatase inhibitors [25 mM Tris.HCl, pH 7.5, 15% glycerol, 20 mM NaF, 170 nM okadaic acid, 2 mM dithiotreitol (DTT), 10 mM β-glycerol phosphate, and 150 μM ATP]. Twenty-microliter aliquots were removed at selected time points and boiled with SDS gel-loading buffer (0.1% bromophenol blue, 50 mM Tris HCl, pH 6.8, 0.1 M DTT, 2% SDS, 10% glycerol) to stop the reaction. At the end of the experiment, 20-μl aliquots were digested with 35 units of calf intestinal phosphatase in buffer (50 mM Tris HCl, pH 7.9, 10 mM MgCl₂, 0.1M NaCl, 1 mM DTT) for 30 min where indicated. All products were analyzed by electrophoresis in 8% SDS–polyacrylamide gels (SDS-PAGE) with an acrylamide:bis-acrylamide ratio of 120:1 to enhance mobility shifts. The gels were fixed and dried and the bands visualized using PhosphorImager screens scanned with Scanner Control SI software (Molecular Dynamics, Sunnyvale, CA).
29. H. Flotow *et al.*, *J. Biol. Chem.* **265**, 14264 (1990).
30. A. Cegielska *et al.*, *J. Virol.* **68**, 269 (1994).
31. N. Dumaz, D. M. Milne, D. W. Meek, *FEBS Lett.* **463**, 312 (1999).
32. K. Sakaguchi *et al.*, *J. Biol. Chem.* **275**, 9278 (2000).
33. J. L. Price *et al.*, *Cell* **94**, 83 (1998).
34. G. A. Keesler *et al.*, *Neuroreport* **11**, 951 (2000).
35. Web text is available at *Science* Online at www.sciencemag.org/cgi/content/full/1057499/DC1.
36. L. J. Ptacek *et al.*, *Cell* **77**, 863 (1994).
37. Single-letter abbreviations for the amino acid residues are as follows: A, Ala; C, Cys; D, Asp; E, Glu; F, Phe; G, Gly; H, His; I, Ile; K, Lys; L, Leu; M, Met; N, Asn; P, Pro; Q, Gln; R, Arg; S, Ser; T, Thr; V, Val; W, Trp; and Y, Tyr.
38. We thank the families who participated in this work, A. Meloni-Ehrig and F. Orfino for technical help, and to G. A. Keesler, E. Vielhaber, and V. Hill for helpful discussions and reagents. Supported by NIH grants HL/HD 59596 (L.J.P.), CA71074 (D.M.V.), and Public Health Service research grant M01-RR00064 from the National Center for Research Resources. L. J. P. is an Investigator of the Howard Hughes Medical Institute.

TRP-PLIK, a Bifunctional Protein with Kinase and Ion Channel Activities

Loren W. Runnels, Lixia Yue, David E. Clapham*

We cloned and characterized a protein kinase and ion channel, TRP-PLIK. As part of the long transient receptor potential channel subfamily implicated in control of cell division, it is a protein that is both an ion channel and a protein kinase. TRP-PLIK phosphorylated itself, displayed a wide tissue distribution, and, when expressed in CHO-K1 cells, constituted a nonselective, calcium-permeant, 105-picosiemen, steeply outwardly rectifying conductance. The zinc finger containing α-kinase domain was functional. Inactivation of the kinase activity by site-directed mutagenesis and the channel's dependence on intracellular adenosine triphosphate (ATP) demonstrated that the channel's kinase activity is essential for channel function.

Phototransduction in *Drosophila* invokes phospholipase C (PLC)–mediated activation of transient receptor potential (TRP) channels, leading to membrane depolarization (*1, 2*). The mammalian TRP channel family may be divided by sequence similarity into short, long, and osm 9–like subfamilies [reviewed in (*3*)]. Receptor-mediated stimulation of PLC activates many members of the short TRP channels, and physical or chemical stimuli activate isoforms of the osm 9–like TRP channel. Long TRP channels (LTRPC), such